

# *Influence of Ni as Minority Alloying Element on the Corrosion Behavior of Amorphous Al-Cu-Mg Alloys in Chloride Solution*

**Vanya Dyakova**  
Materials Testing and Analyses  
IMSTHAC-BAS  
Sofia, Bulgaria  
v\_diakova@ims.bas.bg

**Yoanna Kostova**  
Materials Testing and Analyses  
IMSTHAC-BAS  
Sofia, Bulgaria  
y\_kostova@ims.bas.bg

**Hristina Spasova**  
Materials Testing and Analyses  
IMSTHAC-BASion  
(of Affiliation)  
Sofia, Bulgaria  
h.spasova@ims.bas.bg

**Abstract.** The influence of nickel as minority alloying element on the corrosion behavior of amorphous alloys  $(Al_{74}Cu_{16}Mg_{10})_{99}Ni_1$ ,  $(Al_{74}Cu_{16}Mg_{10})_{98}Ni_2$  and  $(Al_{74}Cu_{16}Mg_{10})_{97}Ni_3$  was investigated. The amorphous alloys were obtained as ribbons by Chill Block Melt Spinning (CBMS). The amorphous structure of the alloys was proven by X-ray diffraction (XRD) and transmission electron microscopy (TEM). The corrosion rate was calculated gravimetric using continuous immersion tests for 360 hours in 3.5% NaCl solution at a temperature of 25°C. The lowest corrosion rate was found in the alloy containing 3 at. % Ni. The chemical composition of the accumulated corrosion products was studied using XRD.

The influence of nickel on the local corrosion resistance of the amorphous ribbons of  $(Al_{74}Cu_{16}Mg_{10})_{100-x}Ni_x$   $x = 0, 1, 2, 3\%$  alloys was investigated electrochemically in a solution of 3.5% NaCl at 25°C. Pitting potential (Epitt) and repassivation potential (Erp) were determined. It was found that most resistant to pitting corrosion was the  $(Al_{74}Cu_{16}Mg_{10})_{97}Ni_3$  alloy, which showed the noblest pitting potential (Epitt -0.332 V) and repassivation potential (Erp -0.530 V).

All obtained corrosion test results of the nickel-containing amorphous alloys were compared to the base amorphous  $Al_{74}Cu_{16}Mg_{10}$  alloy.

**Keywords:** amorphous alloy, aluminum, nickel, copper, magnesium, corrosion.

## I. INTRODUCTION

The first published experimental results on the corrosion properties of amorphous alloys date back to 1974 [1]. From then until now, data have been obtained and analyzed mainly on the corrosion behavior of

amorphous iron-based alloys. The results show that amorphous alloys are more resistant to corrosion than the corresponding crystalline alloys, which can be explained by their microstructural homogeneity, the absence of defects, as well as the positive influence of some of the alloying elements [2], [3].

Aluminium-based amorphous alloys became one of the most studied metallic glasses in the last decades. The influence of various factors on their corrosion resistance continues to be the subject of many studies [4], [5].

The aim of this work is to study the influence of the Ni as a minority alloying element on the corrosion behavior of amorphous alloys  $(Al_{74}Cu_{16}Mg_{10})_{100-x}Ni_x$   $x = 1, 2, 3$  at.% in chloride-containing solution and to estimate their susceptibility to general and local corrosion.

## II. MATERIALS AND METHODS

### A. Methods of Production and Characterization of the Amorphous Ribbons

The  $Al_{74}Cu_{16}Mg_{10}$  alloy was chosen as a base alloy of the Al-Cu-Mg system, corresponding to the eutectic point E5 of the Al-Cu-Mg ternary equilibrium diagram [6]. The base  $Al_{74}Cu_{16}Mg_{10}$  alloy and 1, 2, 3 at.% Ni-containing alloys were synthesized from pure metals Al - 99.99 %, Cu - 99.99 %, Mg - 99.8 % and Ni - 99.99 %, in a plant comprising a resistance electric furnace installed in a water-cooled pneumovacuum chamber in argon atmosphere with 99.998 % purity [7]. The Chill Block

Print ISSN 1691-5402

Online ISSN 2256-070X

<https://doi.org/10.17770/etr2023vol3.7201>

© 2023 Vanya Dyakova, Yoanna Kostova, Hristina Spasova. Published by Rezekne Academy of Technologies.  
This is an open access article under the [Creative Commons Attribution 4.0 International License](https://creativecommons.org/licenses/by/4.0/).

Melt Spinning (CBMS) method was used to obtain rapidly solidified ribbons about 3 - 4 mm wide and 26 - 40  $\mu\text{m}$  thick.

The chemical composition of the produced rapidly solidified ribbons was determined by Energy Dispersive X-ray Spectroscopy (EXDS) using a scanning electron microscope HIROX 5500 with EXDS system BRUCKER. The EXDS results are presented in Table 1.

TABLE 1. CHEMICAL COMPOSITION OF THE RAPIDLY SOLIDIFIED RIBBONS AL-CU-MG-(NI)

Designation of ribbons	Al [at. %]	Cu [at. %]	Mg [at. %]	Ni [at. %]
$\text{Al}_{74}\text{Cu}_{16}\text{Mg}_{10}$	76.60	13.82	9.59	-
$(\text{Al}_{74}\text{Cu}_{16}\text{Mg}_{10})_{99}\text{Ni}_1$	74.45	15.14	9.16	1.24
$(\text{Al}_{74}\text{Cu}_{16}\text{Mg}_{10})_{98}\text{Ni}_2$	74.54	14.90	8.61	1.96
$(\text{Al}_{74}\text{Cu}_{16}\text{Mg}_{10})_{97}\text{Ni}_3$	73.23	14.84	8.72	3.21

X-ray diffraction (XRD) analysis was performed by Bruker D8 Advance powder X-ray diffractometer in order to characterize the amount of amorphous phases of the alloys. The microstructure of the rapidly solidified alloys was studied by transmission electron microscope (TEM) JEOL 1011 at accelerating voltage of 100 kV. The XRD patterns and TEM analyses of the microstructure and TEM diffraction proved that the base alloy  $\text{Al}_{74}\text{Cu}_{16}\text{Mg}_{10}$  was 98 % amorphous [8] and the three Ni – containing alloys (Fig. 1) are completely amorphous [9].

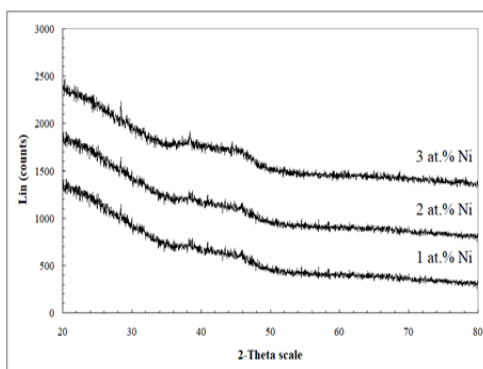


Fig. 1. XRD patterns of  $(\text{Al}_{74}\text{Cu}_{16}\text{Mg}_{10})_{100-x}\text{Ni}_x$  ribbons.

## B. Corrosion Test Methods

### 1. General Corrosion Test

General corrosion tests were performed by continuous immersion of specimens in 3.5% NaCl for 360 hours at a temperature of 25°C in a laboratory thermostat. Before

testing specimens were degreased in acetone and treated in diluted  $\text{HNO}_3$  for one minute.

The corrosion rate (CR) was calculated gravimetrically  $\text{CR} = \frac{\Delta m}{S \cdot t}$  [ $\text{g m}^{-2}\text{h}^{-1}$ ], where the mass loss index  $\Delta m = m_0 - m_1$  [g] was the difference between the weight of the test specimens before the test and after the removal of the corrosion products after the test; S is the surface area of the specimen [ $\text{m}^2$ ]; t is the test duration [h]. The weight testing was made on analytical scales. All obtained CR results are average values from three parallel tests.

After the corrosion test, the specimens were repeatedly washed with warm distilled water. The separated filtrate was dried and analyzed by XRD.

### 2. Potentiodynamic Corrosion Test

The resistance of the studied alloys  $(\text{Al}_{74}\text{Cu}_{16}\text{Mg}_{10})_{100-x}\text{Ni}_x$ ,  $x=0, 1, 2, 3$  at. % to local corrosion was determined by potentiodynamic cyclic method in a solution of 3.5% NaCl at temperature of 25°C. Test specimens of 0.8  $\text{cm}^2$  surface were degreased in alcohol, treated in diluted  $\text{HNO}_3$ . The electrochemical tests were performed in a trielectrode cell with a working electrode made from the studied amorphous alloys, a platinum counter electrode and a silver chloride reference electrode (Ag/AgCl). All potentials in this work are reported relatively to the silver chloride electrode.

The electrochemical tests were performed in a solution of 3.5% NaCl at temperature 25 °C using an Autolab galvanostat-potentiostat model PGSTAT 204 and computer software NOVA 2.1. The results of the polarization tests of studied  $(\text{Al}_{74}\text{Cu}_{16}\text{Mg}_{10})_{100-x}\text{Ni}_x$ ,  $x=1, 2, 3$  at. % alloys were compared to those obtained for the base  $\text{Al}_{74}\text{Cu}_{16}\text{Mg}_{10}$  alloy.

The specimens were kept for 60 min in 3.5% NaCl to stabilize the open circuit potential (OCP), and then were cathodically polarized for 60 s at -0.5V vs OCP to remove the natural passive layer. The cyclic potentiodynamic studies were carried out at scan rate of 1 mV/s in anodic direction from initial potential of -0.5V vs OCP until exceeding the threshold current density with more than 1  $\text{mA}/\text{cm}^2$ , after which the potential scan was reversed in cathode direction to the cross-point of the forward and the backward branches of the polarization curve.

## III. RESULTS AND DISCUSSIONS

### A. General corrosion behavior

The dependence of corrosion rate (CR) on the nickel content of the amorphous alloys  $(\text{Al}_{74}\text{Cu}_{16}\text{Mg}_{10})_{100-x}\text{Ni}_x$ ,  $x=0, 1, 2, 3$  at. % in 3.5% NaCl is shown in Fig. 2. The highest CR is measured for the alloy containing 1 at. % nickel. In the alloys with 2 or 3 at. % Ni the corrosion rate decreases to zero.

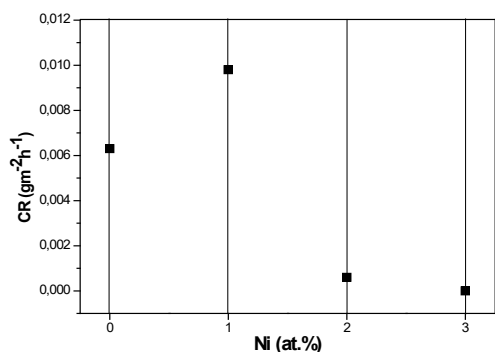
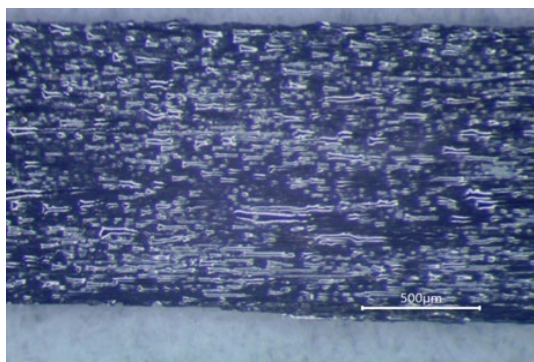
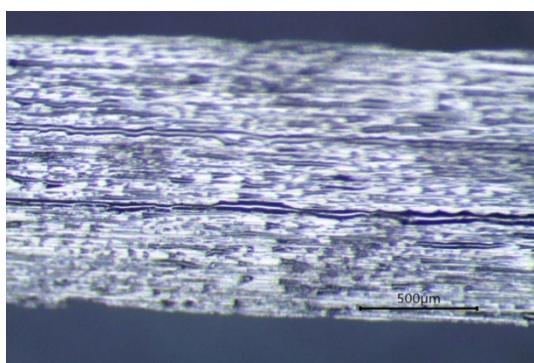


Fig. 2. Corrosion rate CR of  $(Al_{74}Cu_{16}Mg_{10})_{100-x}Ni_x$ ,  $x=0, 1, 2, 3$  at. % alloys under continuous immersion in 3.5 % NaCl for 360 hours at 25°C.

The decrease of CR of the studied alloys with increasing nickel content is explained by the fact that nickel stimulates the formation of passive film on the surface of aluminum alloys, which prevents further interaction of the alloy with the chloride containing aggressive corrosive environment [10]. This is the main reason for the reduction of corrosion losses to zero in the 2 and 3 at. % Ni alloy.



a)  $(Al_{74}Cu_{16}Mg_{10})_{99}Ni$



b).  $(Al_{74}Cu_{16}Mg_{10})_{97}Ni_3$

Fig. 3. Surface of specimens of Ni-containing amorphous alloys after 360 hours corrosion test in 3,5% NaCl at 25°C.

The pitting corrosion is the most common corrosion type of aluminum alloys in chloride solutions [11], [12] but in our case the pittings were absent in all studied Ni-containing amorphous alloys even after 360 hours corrosion test. After the test the surface of the specimens of the alloy with 1 at. % Ni was matte (Fig. 3a), while the surface of the specimens with 3 at. % Ni remained shiny, without separated corrosion products (Fig. 3b), indicating no local corrosion changes.

In order to clarify the possible mechanisms of the corrosion process of Ni-containing aluminum amorphous alloys, the phase composition of the filtrate after washing the test samples was investigated by XRD.

Although no traces of corrosion were visible on the surface of the tested specimens, XRD showed that in addition to NaCl, there were also separated oxide products in the filtrate. (Fig. 4).

An amorphous halo is visible on the onset part of the XRD patterns of the corrosion products of each of the investigated alloys in the region  $(15 \div 25) 2\theta$ , followed by peaks of crystalline phases (Fig.4). This indicates that the released corrosion products are a mixture of amorphous and crystalline type. A similar structure of the layer of corrosion products was observed by other researchers also [13]. The width and the intensity of the amorphous halo at the onset of XRD patterns increases with increasing nickel content in the alloys. Based on our previous research, we can state that the film of corrosion products closest to the metal surface is amorphous mixture of aluminum oxides, oxohydroxides and chlorides [14].

It can be seen from the XRD patterns that the crystal corrosion products contain copper, chlorine and oxygen phases –  $CuCl_2$ ,  $CuO$ , which, according to literature, have good protective corrosion properties [15].

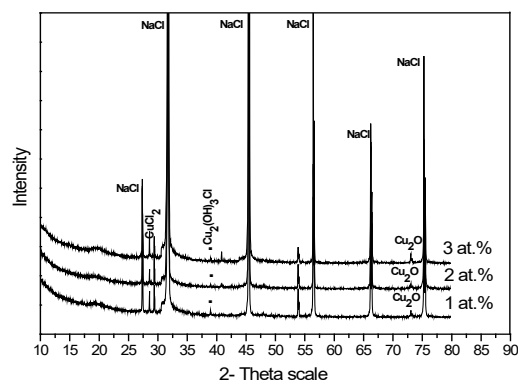


Fig. 4. XRD patterns of the corrosion products of  $(Al_{74}Cu_{16}Mg_{10})_{100-x}Ni_x$  alloys obtained after 360 hours corrosion test in 3.5 % NaCl at 25°C.

### B. Electrochemical and potentiodynamic measurements

Electrochemical corrosion test was performed in order to confirm the results of the general corrosion test and the susceptibility of aluminum amorphous alloys to pitting corrosion.

The method of open circuit potential measurements and potentiodynamic cyclic method were used for the purpose.

The open circuit potentials (OCP) of the base amorphous alloy  $\text{Al}_{74}\text{Cu}_{16}\text{Mg}_{10}$  and of the alloys with 1, 2 and 3 at. % Ni were measured in 3.5 %NaCl at 25°C for 60 min. Figure 5 displays the variations of OCP with the Ni content. Average OCP values are shown in the figure, because in all tested alloys OCP stabilization was not achieved during the 60 min test.

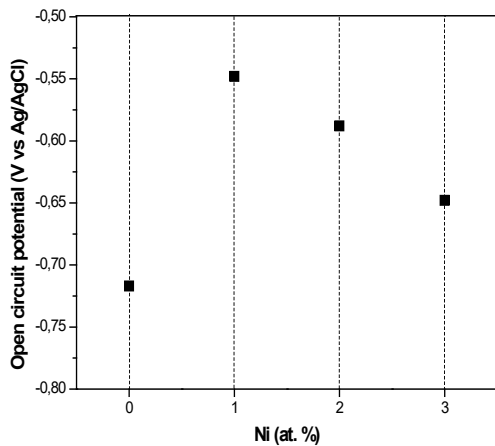


Fig. 5. Dependence of OCP on Ni content of  $(\text{Al}_{74}\text{Cu}_{16}\text{Mg}_{10})_{100-x}\text{Ni}_x$ ,  $x=0, 1, 2, 3$  alloys in 3.5% NaCl at 25°C.

It can be seen that the OCP of all three Ni containing alloys is displaced to less negative values compared to the OCP of the base alloy. The biggest displacement is observed at 1%Ni, the further increase of Ni content diminishes the displacement.

Representative potentiodynamic polarization curves of the amorphous  $(\text{Al}_{74}\text{Cu}_{16}\text{Mg}_{10})_{100-x}\text{Ni}_x$ ,  $x=0, 1, 2, 3$  alloys in 3.5% NaCl are presented in Fig. 6. The pitting potentials  $E_{\text{pit}}$  and the repassivation potentials  $E_{\text{rp}}$  were determined and the values for Ni-containing alloys were compared with  $E_{\text{pit}}$  (solid line) and  $E_{\text{rp}}$  (dotted line) of the base alloy (Fig.7).

The OCPs of the three  $(\text{Al}_{74}\text{Cu}_{16}\text{Mg}_{10})_{100-x}\text{Ni}_x$ ,  $x=1, 2, 3$  at.% Ni alloys (Fig. 5) are more negative than their  $E_{\text{pit}}$  (Fig. 7). The biggest is the difference between OCP and  $E_{\text{pit}}$  in the alloy with 1 at. % Ni. For the base alloy  $\text{Al}_{74}\text{Cu}_{16}\text{Mg}_{10}$ , the values of OCP and  $E_{\text{pit}}$  are close.

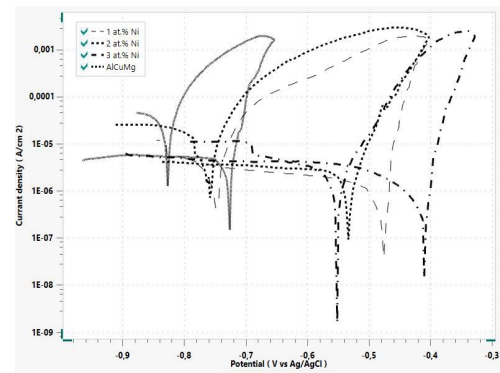


Fig. 6. Polarization potentiodynamic curves of  $(\text{Al}_{74}\text{Cu}_{16}\text{Mg}_{10})_{100-x}\text{Ni}_x$ ,  $x=0, 1, 2, 3$  alloys in 3.5% NaCl at 25°C:  $x=0$ , solid line;  $x=1$ , dash line (- -);  $x=2$ , dot line (.);  $x=3$  dash-dot line (- . - .).

No plateau was registered on the potentiodynamic polarization curves of the amorphous alloys  $(\text{Al}_{74}\text{Cu}_{16}\text{Mg}_{10})_{100-x}\text{Ni}_x$ ,  $x=1, 2, 3$  or the base amorphous alloy  $\text{Al}_{74}\text{Cu}_{16}\text{Mg}_{10}$  in 3.5% NaCl (Fig. 6). Hysteresis loops are formed on the anode part of all polarization curves. The sharp increase of current density immediately after the corrosion potentials ( $E_{\text{corr}}$ ) indicates that the alloys are in a process of active dissolution and their corrosion potentials coincide with their pitting potentials.

When increasing the nickel content in  $(\text{Al}_{74}\text{Cu}_{16}\text{Mg}_{10})_{100-x}\text{Ni}_x$ ,  $x=1, 2, 3$  alloys, the corrosion potential  $E_{\text{corr}}$  shifts in positive direction and the development of pitting corrosion begins. According to Figure 6 the most resistant to pitting corrosion is the  $(\text{Al}_{74}\text{Cu}_{16}\text{Mg}_{10})_{97}\text{Ni}_3$  alloy (dash-dot), which has the noblest pitting potential ( $E_{\text{pit}} -0.332$  V) and repassivation potential ( $E_{\text{rp}} -0.530$  V).

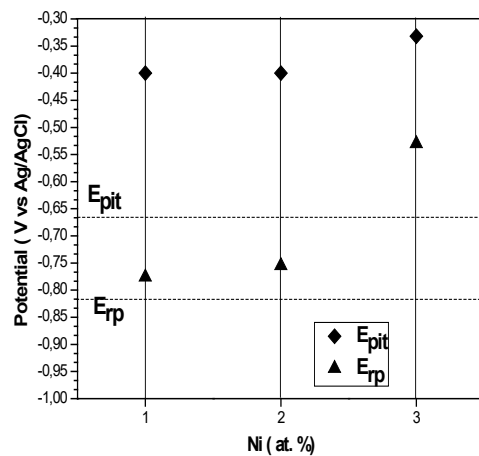


Fig. 7.  $E_{\text{pit}}$  and  $E_{\text{rp}}$  of  $(\text{Al}_{74}\text{Cu}_{16}\text{Mg}_{10})_{100-x}\text{Ni}_x$ ,  $x=1, 2, 3$  at.% and of the base  $\text{Al}_{74}\text{Cu}_{16}\text{Mg}_{10}$  alloy (dot lines).

The base Al<sub>74</sub>Cu<sub>16</sub>Mg<sub>10</sub> alloy for which the highest corrosion current was measured (Fig.2) shows the most negative pitting potential (E<sub>pitt</sub> -0.652 V) and its polarization curve (solid line) is located in the upper part of Fig. 6. The average E<sub>pitt</sub> and E<sub>pr</sub> values of the alloys with different Ni content are presented in Fig. 7. The dotted lines show the E<sub>pitt</sub> and E<sub>pr</sub> of the base alloy Al<sub>74</sub>Cu<sub>16</sub>Mg<sub>10</sub>.

The corrosion behavior of alloys is determined by the difference between the two potentials E<sub>pitt</sub> and E<sub>pr</sub> (Fig. 7). With the increase of Ni content in (Al<sub>74</sub>Cu<sub>16</sub>Mg<sub>10</sub>)<sub>100-x</sub>Ni<sub>x</sub>, x=1,2,3 amorphous alloys the zone between E<sub>pitt</sub> and E<sub>pr</sub> narrows and the zone of their cathodic potentials where they are corrosion protected expands (Fig. 6). The results indicate that most protected from pitting corrosion is the alloy (Al<sub>74</sub>Cu<sub>16</sub>Mg<sub>10</sub>)<sub>97</sub>Ni<sub>3</sub>.

#### IV. CONCLUSIONS

It was found that the addition of nickel in the range of 2-3 at % to the base amorphous alloy Al<sub>74</sub>Cu<sub>16</sub>Mg<sub>10</sub> reduces the corrosion rate of the amorphous alloys (Al<sub>74</sub>Cu<sub>16</sub>Mg<sub>10</sub>)<sub>100-x</sub>Ni<sub>x</sub>, x=2,3 from 63.10<sup>-4</sup> [g m<sup>-1</sup> h<sup>-1</sup>] to 0 [g m<sup>-1</sup> h<sup>-1</sup>]

The addition of nickel in the range of 1-3 at % to the base amorphous alloy Al<sub>74</sub>Cu<sub>16</sub>Mg<sub>10</sub> increases the resistance of the amorphous alloys (Al<sub>74</sub>Cu<sub>16</sub>Mg<sub>10</sub>)<sub>100-x</sub>Ni<sub>x</sub>, x=1, 2, 3 to pitting corrosion in a chloride-containing solution.

#### ACKNOWLEDGEMENTS

This study is funded by the project "Study of the rheological and corrosion behavior of amorphous and nanocrystalline aluminum-based alloys", Contract with BNSF №KP-06-H37/13 of 06 December 2019.

A part of experimental units used in this work was funded by the European Regional Development Fund within the OP "Science and Education for Smart Growth 2014 - 2020", project CoE "National center of mechatronics and clean technologies", No BG05M2OP001-1.001-0008-C08.

#### REFERENCE

[1] M. Naka, K. Hashimoto, T. Masumoto, J. Japan Inst. Metals, vol. 38, pp.835-841, 1974.  
[2] T. Aburada, N. Uēnlūē, J.M. Fitz-Gerald, G.J. Shiflet and J.R. Scully, "Effect of Ni as a minority alloying element on the

corrosion behavior in Al-Cu-Mg-(Ni) metallic glasses," Scripta Materialia, vol.58, pp. 623-626, 2008, <https://doi.org/10.1016/j.scriptamat.2007.11.041>  
[3] S. Dhasneem, S. S. Farhana, S. Rajendran, T. Umasankareswari, S. Shanmugapriya, D. Renita, "Corrosion resistance of metallic glasses", International journal of nano corrosion science and engineering, vol. 3, no. 1, pp. 48-59, 2016.  
[4] A. Kukuła-Kurzyniec, J. Dutkiewicz, P. Ochinn, L. Perriere, P. Dhuzewski, A. Góral, "Amorphous - nanocrystalline melt spun Al-Si-Ni based alloys modified with Cu and Zr." Archives of Metallurgy and Materials, vol. 58, no.2, pp. 419-423, 2013, DOI: 10.2478/amm-2013-0010.  
[5] Y.Q. Cheng, E. Ma, 'Atomic-level structure and structure-property relationship in metallic glasses,' Progress in Materials Science, vol. 56, pp. 379-473, doi:10.1016/j.pmatsci.2010.12.002.  
[6] Ternary Al-Cu-Mg diagram MSIT Workplace, <https://www.msiport.com/msi-research/ternary-evaluations/notes-for-authors-pdf/>, ID:10.12587(2003).  
[7] M. Gögebakan, O. Uzun, T. Karaaslan, M. Keskin, "Rapidly solidified Al-6.5 wt. % Ni alloy", Journal of Materials Processing Technology, vol. 142, no.1, pp. 87-92,2003,<https://www.sciencedirect.com/science/article/abs/pii/S0924013603004667>.  
[8] V. Dyakova, G. Stefanov, I. Penkov, D. Kovacheva, N. Marinkov, Y. Mourdjeva, S. Gyurov, "Influence of Zn on glass forming ability and crystallization behaviour of rapidly solidified Al-Cu-Mg (Zn) alloys", Journal of Chemical Technology and Metallurgy, vol. 57, no. 3, pp. 622-630, 2022, [https://dl.uctm.edu/journal/node/j2022-3/23\\_21-64\\_br\\_3\\_pp\\_622-630.pdf](https://dl.uctm.edu/journal/node/j2022-3/23_21-64_br_3_pp_622-630.pdf).  
[9] V. Dyakova, Y. Mourdjeva, N. Marinkov, G. Stefanov, Y. Kostova, S. Gyurov, "Effect of Ni as minority alloying element on glass forming ability and crystallization behavior of rapidly solidified Al-Cu-Mg-Ni ribbons", Journal of Chemical Technology and Metallurgy - in print.  
[10] G. S. Frankel, M. A. Russak, C.V. Jahnes, M. Mirzamaani, V.A. Brusic, "Pitting of Sputtered Aluminum Alloy Thin Films", J. Electrochem. Soc., vol. 136, no. 4, pp.1243-1244, 1989, DOI: <https://doi.org/10.1149/1.2096864>.  
[11] V. Harshmeet, "The corrosion behaviour of aluminium alloy b206 in seawater", M.S. thesis, University of British Columbia, Vancouver, 2016.  
[12] R. Orozco, J. Genesca, J.Juarez-Islas, "Effect of Mg Content on the Performance of Al-Zn-Mg Sacrificial Anodes", ASM Internat. JMEPEG, no. 16, p. 229-235, 2007, DOI:10.1007/s11665-007-9037-z.  
[13] V. Dyakova, Y. Kostova, S. Gyurov, D. Kichukova, H. Spasova, "The influence of Zn on the corrosion behaviour of amorphous and nanosized rapidly solidified (Al<sub>75</sub>Cu<sub>17</sub>Mg<sub>8</sub>)<sub>100-x</sub>Ni<sub>x</sub> alloys and their crystalline analogues", Mater. Sci. Non-Equilib. Phase Transform., vol. 6, no.3, pp. 73-76, 2020, <https://stumejournals.com/journals/ms/2020/3/73.full.pdf>  
[14] V. L. Dyakova, Y. G. Kostova, B. R. Tzaneva, "Effect of minority alloying elements Zn and Zr on the corrosion behavior of amorphous alloys AlCuMg(Zn) and AlCuMg(Zr) and their nanocrystalline analogues," ChemChemTech, vol. 65, no. 4, pp. 62-70, 2022, DOI: <https://doi.org/10.6060/ivkkt.20226504.6550>.  
[15] K. Dževad, K. Kozlica, J. Ekar, J. Kovač, and I. Milošev, "Roles of chloride ions in the formation of corrosion protective films on copper," Journal of The Electrochemical Society, vol.168, p. 031504, 2021, DOI:10.1149/1945-7111/ABE34A.